JOURNAL OF SOLID STATE CHEMISTRY 80, 80–93 (1989)

Space Group of U_4O_9 in the Beta Phase

J. P. LAURIAT*,‡ AND G. CHEVRIER†

Cristallographie et Physique des Matériaux, Université Paris-Sud, 91405 Orsay Cedex, France

AND J. X. BOUCHERLE

Centre d'Etudes Nucléaires DRF/SPH-MDN, 85X, 38041 Grenoble Cedex, France

Received July 16, 1987; in revised form December 22, 1988

A single-crystal U_4O_9 has been examined by neutron diffraction above the transition temperature at 120°C; two data sets have been collected at 1.18 and 0.84 Å. Also the variation of the intensities of selected reflections have been investigated across the transition. The space group $I\bar{4}3d$ of the U_4O_9 superlattice is confirmed just above the transition temperature. The data are analyzed using a U_6O_{37} cluster model and a statistical model, obtained by superimposing the content of a $4a \times 4a \times 4a$ supercell inside an averaged cell $a \times a \times a$. Above the transition temperature it appears that, on the average, about 80% of oxygen atoms remain in their fluorite UO_2 sites, and that the additional oxygen atom and 20% of the normal oxygen atoms occupy new sites (O′) and (O″) corresponding to displacements along [110] and [111], respectively, from the cubic coordinates sites. It is found that the uranium atoms remain undisturbed at their fluorite positions. Above the phase transition, the oxygen atoms have the tendency to form complex defects in which the (O′) displaced oxygen atoms and the vacancies in the oxygen sublattice are dominant. Consequently, the U_4O_9 phase can be interpreted, not as a systematic insertion of oxygen ions in the vacant sites of the fluorite structure, but rather as a rebuilding of the UO_2 structure.

Introduction

Uranium dioxides in the range UO_2–U_3O_8 have been the subject of intensive investigations (*1, 2*). At the composition $UO_{2.25}$ the oxygen atoms are ordered to form a new phase U_4O_9, which has been observed by X-ray (*3*), neutron (*4*), and electron (*5*) diffraction patterns.

In an X-ray Debye–Scherrer photograph, "main" (or "fundamental") reflections corresponding to a well-crystallized UO_2 oxide are observed, as are additional superlattice reflections which are much weaker than the fundamental ones and prominent only at great Bragg angles. All of these reflections can be indexed in a $4a \times 4a \times 4a$ cubic cell where $a = 5.44$ Å is the parameter of the UO_2-type pseudocell.

U_4O_9 undergoes a rhombohedral-to-cubic phase transformation in a temperature interval from 60 to 90°C. This phase transition has already been detected on the basis of several experiments: contraction in the

* Present address: Lure, Bâtiment 209 C, Université Paris-Sud, 91405 Orsay Cedex, France.

† Present address: L.L.B. Spectrométrie neutronique, C.E.N. Saclay, F 91191 Gif sur Yvette Cedex, France.

‡ To whom correspondence should be addressed.

0022-4596/89 $3.00

lattice constant (*6, 7*), anomaly of the specific heat (*8*), and differential thermal analysis (*9*). Belbeoch *et al.* (*6*) reported that the symmetry is rhombohedral at room temperature (a = 5.4483 Å, α = 90.078 ± 0.002°) and becomes cubic above the transition temperature, which occurs at (65 ± 10)°C for pure U_4O_9.

On the basis of systematic extinctions observed on a Weissenberg diagram, Belbeoch *et al.* (*3*) proposed the space group $I\bar{4}3d$ for U_4O_9 at room temperature. Willis (*4*) confirmed this group by neutron diffraction on single crystal as did Blank and Ronchi (*5*) by electron diffraction, always at room temperature. Later, Belbeoch *et al.* (*6*) proposed that U_4O_9 be considered in space group $I\bar{4}3d$ only above the transition temperature. Nevertheless, Masaki and Doi (*10*), using *hk*0 neutron data indicated the space group $I4_13d$. Masaki (*11*) confirmed this space group above the transition temperature. It has been now well established that U_4O_9 crystallizes in a body-cubic-centered structure but there is some uncertainty in the literature about the correct cubic space group above the transition temperature.

The detailed atomic arrangement in U_4O_9 remains presently unknown. Indeed, some discrepancies between the conclusions proposed in the literature are not surprising due to uncertainties about the U_4O_9 single-crystal preparation, to the actual accuracy needed when measuring the intensities of selected reflections, and in addition to the inherent difficulties associated with the U_4O_9 structure. It seems worthwhile to measure neutron diffraction intensities of selected reflections in order to clarify the following points: (i) space group above the transition, (ii) change in intensities of main and superlattice reflections at the transition, (iii) test of structural models earlier proposed by several authors, but above the transition temperature and on the basis of data sets including superlattice reflections.

Structural Models of U_4O_9

The interstitial models are based on ordered occupancies of interstitial sites in the $UO_2(U_4O_8)$ considered as a mother structure for the U_4O_9 phase. As a reminder, UO_2 has the fluorite structure with oxygen atoms at the (0 0 0; FC) and ($\frac{1}{2}$ $\frac{1}{2}$ $\frac{1}{2}$; FC) positions of the cubic cell (space group $Fm3m$) and the uranium atoms at the ($\frac{3}{4}$ $\frac{3}{4}$ $\frac{3}{4}$; FC) positions. The extra oxygen atoms are inserted, at the rate of one per unit cell, in the cubic coordinated sites located at ($\frac{1}{4}$ $\frac{1}{4}$ $\frac{1}{4}$; FC) positions. Two interstitial models have already been investigated. First, Belbeoch *et al.* (*3*) proposed one systematic insertion of the extra oxygen atoms based on the $\bar{4}$ repetition law and obtained an ideal arrangement belonging to the space group $I\bar{4}3d$. So, they arranged the 832 atoms within the large cell (256 uranium atoms, 512 oxygen atoms, and 64 extra oxygen atoms) in ideal positions. The complete determination of the structure requires the knowledge of the displacements of 808 atoms from their ideal positions (24 are in fixed positions). On the basis of the X-ray extinctions observed at room temperature they concluded that all of the 64 extra oxygen atoms can be displaced only along the [111] directions. Second, Masaki and Doi (*10*) and later Masaki (*11*) analyzed neutron intensities of *hk*0-type superlattice reflections on the basis of the $I4_132$ space group. Forty extra oxygen atoms are found at the center of cubic coordinated sites, whereas 24 are displaced by 0.52 Å along [110] directions from these sites. Sixteen uranium atoms out of the 256 located in the supercell are found to be displaced by 0.45 Å from their positions in the fluorite-type structure.

The U_6O_{37} cluster model predicts the existence of U_6O_{37} groups derived from the U_6O_{32} blocks appearing in the UO_2 structure. In the fluorite MX_2 structure, each cation M is coordinated by a cube of eight X anions. The M_6X_{32} block is made up of six

filled anionic X_8 cubes which surround an empty X_8 cube, each cube having in common one face of the central cube. S. Aleonard *et al.* (*12*) and Bevan *et al.* (*13*) have observed that the X_8 anionic cube is transformed into a square antiprism when a few extra anions are put into a fluorite-related compound. The U_6O_{36} structural unit is derived from the U_6O_{32} group by 45° rotations, around each fourfold axis, of the only faces shared with the central empty cube. As a consequence of the rotation, this inner cube (8 vertices) is converted into an empty cuboctahedron (12 vertices). The four vacant sites are occupied with the extra oxygen atoms, and the filling of the center of the cuboctahedron by a fifth extra-oxygen atom gives rise to the U_6O_{37} group. So, the existence of an isolated U_6O_{37} cluster in the U_4O_9 structure involves a distribution of U cations in 8- through 10-fold coordination. The model proposed by Bevan *et al.* (*14*) is based on an arrangement of 12 isolated U_6O_{37} clusters within the large cell centered on $\bar{4}$ axis, on the 12-fold positions of the $I\bar{4}3d$ space group. The positions of 256 uranium atoms and 572 oxygen atoms (theoretical composition $UO_{2.234}$) are determined from the analysis of single crystal neutron diffraction data collected at 230 and 500°C. An R factor of 16% is obtained with four variable positional parameters.

The statistical analysis for the uranium oxide was the starting point from which some cluster models were issued. Willis (*4*) proposed a statistical model where the interstitial oxygen ions are in association with oxygen vacancies and uranium ions.

A statistical model involving long-range ordering of oxygen complexes has been proposed by Willis (*4*). The neutron diffraction intensities on single crystals are analyzed on the basis of an average unit cell $a \times a \times a$ obtained by superposing the 64 subcells inside the $4a \times 4a \times 4a$ supercell. Within this average cell, the uranium atoms occupy exactly the positions they have in the UO_2 cell, three types of oxygen atoms O, O′, and O″ are present. The O atoms occupy the same type of sites as the oxygen atoms in UO_2 but a proportion of these sites are empty; the O′ and O″ atoms occupy interstitial sites, which are found displaced by about 1 Å along [110] for O′ and along [111] for O″ from the cubic coordinated sites; the holes themselves are unoccupied. Willis deduced the occupation number of oxygen atoms and the magnitude of displacements in the average unit cell only from the main reflections, measured at room temperature.

Experimental

The sample is a single-crystal sphere, having a diameter of 2.0 mm and a weight of 49.6 mg, supplied by General Electric Co. (1962), oxidized, and ordered by B. Belbeoch. The parameter corresponding to the measured O/U ratio is 21.77 Å. The sphere is sealed in a Lindeman capillary with a 0.01-mm wall for the neutron experiments, to avoid reoxidizing and thus the change of the O/U ratio; it is oriented by X-ray diffraction with a [111] axis placed perpendicular to the incident beam. The neutron absorption is small enough ($\mu R < 0.02$) to be neglected for corrections. We verified that the empty capillary does not significantly affect the background. The scattering lengths used for uranium and oxygen atoms were $b_u = 0.84 \times 10^{-12}$ and $b_0 = 0.58 \times 10^{-12}$ cm, respectively.

Several runs of data collection have been performed on a 4-circle diffractometer installed at Siloé reactor (35 MW, thermal neutrons) and at Orphée reactor (14 MW, hot source) of L.L.B. with the same experimental setup for both diffractometers: the incident beam had an 8-mm cross section, a 20-mm reception diaphragm corresponding to an angular range equal to 3.6°, and scanning steps at intervals of 0.05° for every in-

tensity measurement. Three wavelengths have been used for these studies:

—λ = 1.12 Å from a 311 germanium monochromator; $\lambda/2$ contamination lower than 10^{-5} (C.E.N. Grenoble-Siloé reactor).

—λ = 1.176 Å from a 220 copper monochromator; $\lambda/2$ contamination lower than 5×10^{-3} (C.E.N. Grenoble-Siloé reactor).

—λ = 0.84 Å from a 220 copper monochromator and a 0.25-mm Erbium filter: $\lambda/2$ contamination lower than 10^{-4} (L.L.B. Orphée reactor).

A device utilizing a hot air stream as heater has been installed on both diffractometers in order to scan the temperature around the transition temperature. Some details of this equipment, specially built for these diffraction experiments, are given in the Appendix.

Results

(*i*) *Phase Transition*

A U_4O_9 powder sample has been prepared in the same manner as described by Belbeoch *et al.* (*6*) with an atomic ratio O/U equal to (2.244 ± 0.005). Its analysis by differential scanning calorimetry (DSC, Perkin–Elmer) shows an endothermic peak taking place in a temperature interval from 50 to 90°C, as the temperature increases or decreases (Fig. 1). After calibration of the apparatus and corrections of thermal inertia (*15*), we obtain the transition temperature 72 ± 1°C and the increment of enthalpy with the transition 0.4 cal/g. This value is comparable to that associated with the anomaly of the heat capacity (0.62 cal/g – 8).

The transition temperature range and the change in the intensity of typical reflections at the transition have been investigated by means of single-crystal neutron diffraction. The plots of integrated intensity against temperature of the 880 and 0024 main reflections are shown in Fig. 2 as an example. The transition temperature range extends from 60 to 100°C and the transition temperatures measured at half variation (69 ± 3 and 72 ± 3°C, respectively) are in good agreement with the results obtained by

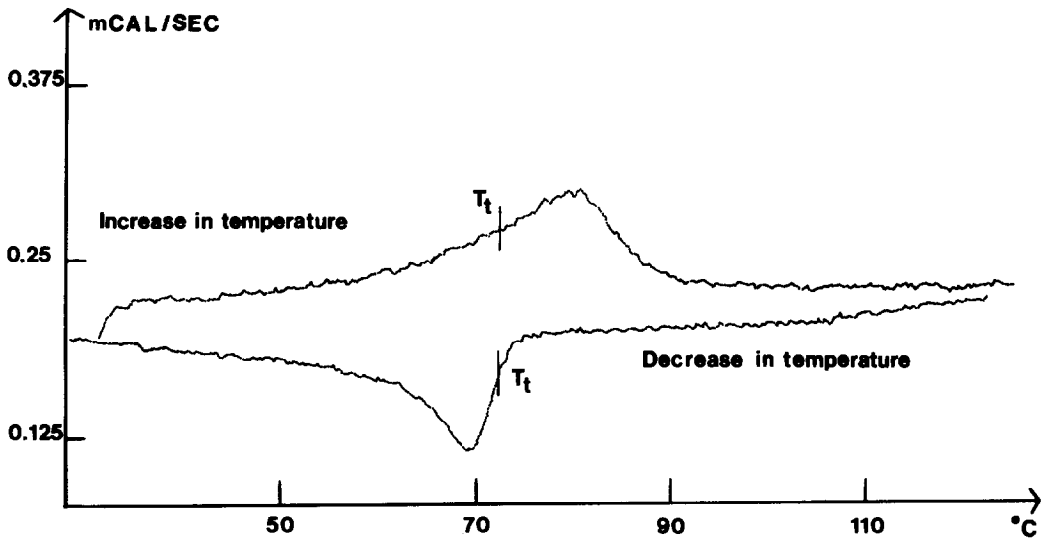

FIG. 1. Variation of enthalpy of a U_4O_9 powder sample weighing 17 mg, registering at a scan rate of 10°/min.

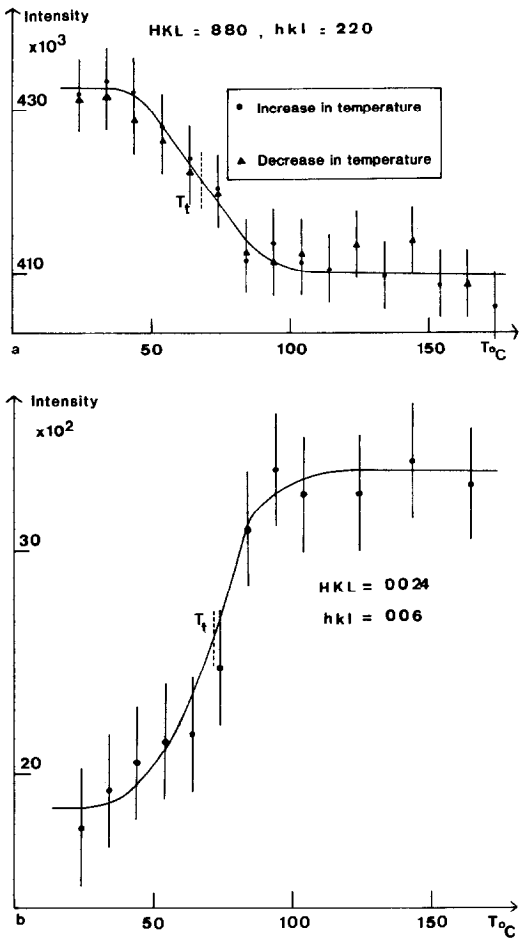

FIG. 2. Integrated intensity as a function of tempera ture in the region of the transition, for a strong (a) and a weak (b) main reflection.

DSC technique. These values correspond to pure U_4O_9 phase without U_3O_8 or UO_2 trace, as reported by Naito *et al.* (*7*). As a conclusion, it is necessary to raise the temperature of the U_4O_9 sample to at least 100°C in order to investigate its structure above the transition.

Some authors reported a considerable change in intensity of reflections at the transition, on the basis of neutron diffraction (*7*) and X-ray diffraction (*6*) on a powder sample. We measured the magnitude of intensity variations occurring between room temperature and 120°C, averaging over at least three equivalent reflections. The results are summarized in Table I. Subsequently, the working temperature above the transition temperature was fixed at 120°C. The changes in intensities of reflections at the transition does not follow any rule clearly. Roughly, the strong and medium main reflections decrease while the superlattice ones increase.

(*ii*) *Space Group above the Transition Temperature*

The space group $I4_132$ distinguishes itself from the space group $I\bar{4}3d$ by the *hhl* reflections, which exist in $I\bar{4}3d$ only if $2h + l = 4n$. So, Masaki and Doi (*10*) justified the space group $I4_132$ by 770 and 990 reflections.

By ω-scanning with a 1.12 Å wavelength (Siloé reactor), we have not observed a peak in 770 and 990 positions and, in addition, by ω-2θ scanning of the 110 reciprocal row, with a 1.18 Å wavelength (Siloé reactor), no peak is found at the *hh*0 positions with $h = 2n + 1$ up to $h = 19$ as illustrated in Fig. 3. The small peak observed at $h = 5.35$ does not correspond to any reciprocal lattice point of the [110] reciprocal row; it is due to the experimental setup and presumably corresponds to the tails of the fundamental 800 reflection. We have not found the weak but distinct peaks in (9.5, 9.5, 0) and (10.5, 10.5, 0) also reported by Masaki and Doi (*16*) either. In conclusion, our measurements are in agreement with the X-ray studies performed earlier by Belbeoch *et al.* (*3*) and confirm the space group of $I\bar{4}3d$ which they proposed.

(*iii*) *Intensity Measurements*

Two data sets have been collected at 120°C: 67 reflections up to $\sin\theta/\lambda = 0.45$ Å^{-1} (1.18 Å, Siloé reactor) and 82 reflections up to $\sin\theta/\lambda = 0.72$ Å^{-1} (0.84 Å, Orphée reactor). The integrated intensities

TABLE I

VARIATION OF INTENSITY ACROSS THE TRANSITION

$H^2 + K^2 + L^2$	H K L	h k l	$(I_{120} - I_{20})/I_{20}$	Ecart type
Main reflections $h + k = l = 4n$ (Siloé, 1.12 Å)				
128	8 8 0	2 2 0	−0.077	0.06
Main reflections $h + k + l = 4n$ (Siloé, 1.18 Å)				
128	8 8 0	2 2 0	−0.066	0.05
256	16 0 0	4 0 0	−0.050	0.02
384	16 8 8	4 2 2	−0.017	0.03
512	16 16 0	4 4 0	−0.098	0.02
640	24 8 0	6 2 0	−0.028	0.01
Main reflections $h + k + l = 4n \pm 1$ (Siloé, 1.12 Å)				
48	4 4 4	1 1 1	−0.082	0.02
Main reflections $h + k + l = 4n \pm 1$ (Siloé, 1.18 Å)				
48	4 4 4	1 1 1	−0.076	0.02
176	12 4 4	3 1 1	+0.020	0.02
304	12 12 4	3 3 1	+0.033	0.01
432	20 4 4	5 1 1	−0.037	0.01
432	12 12 12	3 3 3	−0.227	0.01
560	20 12 4	5 3 1	+0.031	0.01
Main reflections $h + k + l = 4n + 2$ (Siloé, 1.12 Å)				
64	8 0 0	2 0 0	+1.105	0.05
192	8 8 8	2 2 2	−0.228	0.05
Main reflections $h + k + l = 4n + 2$ (Siloé, 1.18 Å)				
64	8 0 0	2 0 0	+0.357	0.5
192	8 8 8	2 2 2	0.000	0.2
320	16 8 0	4 2 0	+0.214	0.2
576	16 16 8	4 4 2	+0.198	0.1
576	24 0 0	6 0 0	+0.912	0.6
Superlattice reflections (Siloé, 1.12 Å)				
16	4 0 0	1 0 0	−0.545	0.4
24	4 2 2		−0.071	0.8
32	4 4 0	1 1 0	+1.403	0.2
42	5 4 1		+1.478	1.0
72	6 6 0		+1.344	0.2
86	6 5 5		+1.011	0.06
86	7 6 1		+5.710	0.7
90	9 3 0		+0.344	0.05
102	7 7 2		−0.483	0.03
102	10 1 1		+0.441	0.05
104	10 2 0		+0.577	0.05
122	9 5 4		+2.689	1.3
122	11 1 0		+0.876	0.06
144	12 0 0	3 0 0	+3.523	0.3

are taken on an average of at least three equivalent reflections, and the associated standard deviations were calculated with the aid of the ARRNGE program for correction (*17*). The reflections contaminated by $\lambda/2$ were rectified. The structure factors $|F_{obs}|$, classified into *hkl* groups, are listed in Table II at the same scale; they are taken as unobservable, i.e., equal to 0 if $|F_{obs}| < 2$ sig(F_{obs}). The following facts can be stated:

(A) A comparison of data collected with 1.18- and 0.84-Å wavelengths gives an R_1 factor of 1% where R_1 is defined by $R_1 = \Sigma||F_{gj}| - |F_{bj}||/\Sigma|F_{bj}|$. The structure factors are $|F_{gj}|$ at 1.18 Å and $|F_{bj}|$ at 0.84 Å; j represents the jth observed structure factor corresponding to the same *hkl* values in Table II. This value of R_1 suggests that these measurements are not subject to systematic errors from secondary extinction. Willis (*4*) reported that the entry of oxygen atoms in UO_2 increases the mosaic spread to a point at which the extinction is not appreciable.

(B) The differences in intensities of nonequivalent *hkl* reflections which occur at the same values of $h^2 + k^2 + l^2$ (as 333 and 511, for example) reach a maximum of 40%, much larger than the difference observed in UO_2 oxide (*18*).

(C) The superlattice reflections show a wide range of intensities, from one-tenth to one-hundredth of the intensities of the $4n$ main reflections.

(D) We find that superlattice reflections (as reported in Table II) whose indices are $h, k, l = 8n \pm 1$, $8n \pm 1$, $4n$ and $8n \pm 3$, $8n \pm 3$, $4n$ are unobservable without exception. These indices correspond to the extinction rules of the 12a, 12b positions for the space group $I\bar{4}3d$ (positions with symmetry $\bar{4}$).

Testing of Models above the Transition Temperature

The difference observed between the theoretical density of U_4O_9, 11.29 g/cm^3, and the measured density, 11.20 g/cm^3 (*3*), could be due to a maximum of one or two uranium vacancies associated with three or six oxygen vacancies within the $4a \times 4a \times 4a$ cell. But, on the other hand, the nonsymmorphic $I\bar{4}3d$ space group does not allow a Wyckoff site with a multiplicity of less than 12. Consequently, a U_4O_9 structure having uranium vacancies is not consistent with the density measurements.

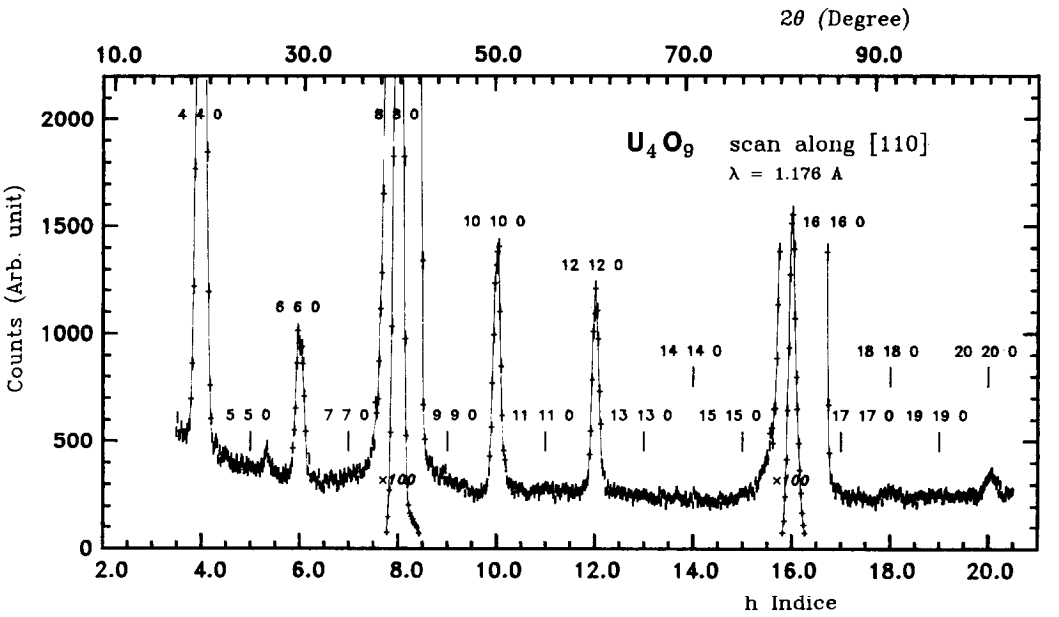

FIG. 3. ω-2θ scan along the $h\,h\,0$ reciprocal line at 120°C. Main reflections: 8 8 0 and 16 16 0. Superlattice reflections: indices $h = 2n$. Reflections of the type $(h, h, 0)$ with $h = 2n + 1$ are not observed.

Interstitial Structural Models

These models can be classified into groups depending on atoms set in the special positions with symmetry $\bar{4}$ (Wyckoff sites 12a, 12b with fixed coordinates of the space group $I\bar{4}3d$): either a normal oxygen atom, a uranium atom, or an extra oxygen atom. After a methodical analysis, Perio (*19*) counted 15 independent models, including the model early obtained by a systematic distribution of extra oxygen atom (*3*).

We selected only the model appearing in better agreement with the diffraction results, which is characterized as follows: (i) 24 uranium atoms are located at the positions with symmetry $\bar{4}$; (ii) 16 extra oxygen atoms occupy positions corresponding to corners and centers of $2a \times 2a \times 2a$ cubes; (iii) the 48 remaining extra oxygen atoms are placed at positions where they form 12 regular tetrahedrons centered on the positions surrounding the uranium atoms. At last, the supercell contains 808 atoms out of 832 located in the 48, 24, 16 atoms of Wyckoff groups with nonfixed coordinates.

The displacements δx, δy, δz from these ideal positions are parameters introduced in refinement. However, to reduce the number of independent parameters, we have supposed that uranium and normal and extra oxygen atoms relax without changing the form of tetrahedrons and cubes where they are located. With this constraint, the displacements are taken as $|\delta x| = |\delta y| = |\delta z|$ and there are no more than 15 displacement parameters instead of 49. Refinement was done by a least-squares process using XFLSN program (*20*). The R factor, $R = \Sigma||F_{oj}| - |F_{cj}||/\Sigma|F_{oj}|$, determined from 65 observed reflections (Orphée data collection) did not go below 0.19.

U_6O_{37} Cluster Model

We tested the structural model proposed by Bevan *et al.* (*14*). The arrangement of the 12 discrete U_6O_{37} groups in the $4a \times 4a \times 4a$ cell is consistent with the observation

TABLE II

Neutron Diffraction Data

$H^2+K^2+L^2$	$H\ K\ L$	$h\ k\ l$	$\lvert F\rvert_{\text{Orphée}}$	$\sigma_{\text{Orphée}}$	$\lvert F\rvert_{\text{Siloé}}$	$\sigma_{\text{Siloé}}$
	Main reflections $h+k+l=4n$					
128	8 8 0	2 2 0	640	5	615	5
256	0 0 16	0 0 4	557	3	545	3
384	8 8 16	2 2 4	544	3	537	3
512	16 16 0	4 4 0	—	—	475	3
640	24 8 0	6 2 0	—	—	455	3
768	16 16 16	4 4 4	493	4	—	—
896	24 16 8	6 4 2	369	3	—	—
1024	0 0 32	0 0 8	425	3	—	—
1152	32 8 8	8 2 2	336	3	—	—
1152	0 24 24	0 6 6	334	1	—	—
1280	0 16 32	0 4 8	283	2	—	—
1408	16 24 24	4 6 6	270	2	—	—
1536	16 16 32	4 4 8	216	2	—	—
	Main reflections $h+k+l=4n+1$					
48	4 4 4	1 1 1	259	2	260	2
176	4 4 12	1 1 3	330	2	332	2
304	12 12 4	3 3 1	309	2	310	2
432	12 12 12	3 3 3	243	1	244	2
432	4 4 20	1 1 5	307	2	306	2
560	20 12 4	5 3 1	—	—	283	2
688	12 12 20	3 3 5	212	2	212	1
816	4 4 28	1 1 7	212	1	—	—
816	20 20 4	5 5 1	248	1	—	—
944	4 12 28	1 3 7	239	1	—	—
944	20 20 12	5 5 3	202	1	—	—
1072	12 12 28	3 3 7	237	2	—	—
1200	4 20 28	1 5 7	214	2	—	—
1200	20 20 20	5 5 5	154	2	—	—
1328	4 4 36	1 1 9	160	2	—	—
1328	12 20 28	3 5 7	189	2	—	—
1408	4 12 36	1 3 9	174	1	—	—
1536	12 12 36	3 3 9	166	2	—	—
1584	28 28 4	7 7 1	138	3	—	—
1584	20 20 28	5 5 7	171	2	—	—
	Main reflections $h+k+l=4n+2$					
64	0 0 8	0 0 2	31	3	34	4
192	8 8 8	2 2 2	19	1	21	3
320	16 8 0	4 2 0	26	2	25	1
576	0 0 24	0 0 6	58	1	62	6
576	16 16 8	4 4 2	75	1	76	1
704	8 8 24	2 2 6	50	1	—	—
832	0 16 24	0 4 6	46	1	—	—
1088	32 8 0	8 2 0	96	1	—	—
1088	16 16 24	4 4 6	104	1	—	—
1216	24 24 8	6 6 2	87	1	—	—
1344	32 16 8	8 4 2	63	1	—	—
1600	0 0 40	0 0 10	81	1	—	—
1600	0 24 32	0 6 8	94	1	—	—
1728	24 24 24	6 6 6	98	1	—	—
1728	8 8 40	2 2 10	79	1	—	—
	Superlattice reflections $H00$					
16	4 0 0	1 0 0	5	2	—	—
144	12 0 0	3 0 0	28	1	28	1
324	18 0 0		0	1	—	—
400	20 0 0	5 0 0	46	1	45	1
784	28 0 0	7 0 0	—	—	6	3
	Superlattice reflections $HH0$					
32	4 4 0	1 1 0	18	1	—	—
72	6 6 0		20	1	—	—
200	10 10 0		35	1	—	—
288	12 12 0	3 3 0	25	1	—	—
392	14 14 0		14	1	—	—
648	18 18 0		16	1	—	—
800	20 20 0	5 5 0	16	2	13	1
	Superlattice reflections $HK0$					
80	4 8 0	1 2 0	9	2	—	—
90	3 9 0		—	—	26	1
104	2 10 0		—	—	40	1
106	5 9 0		—	—	56	1
122	11 1 0		—	—	61	1
160	12 4 0	3 1 0	11	1	—	—
208	12 8 0	3 2 0	22	1	—	—
244	12 10 0		—	—	57	1
272	16 4 0	4 1 0	6	2	8	1
290	17 1 0		—	—	0	1
298	17 3 0		—	—	64	1
400	16 12 0	4 3 0	15	1	16	1
404	20 2 0		—	—	56	1
416	20 4 0	5 1 0	10	1	18	1
464	20 8 0	5 2 0	8	2	—	—
544	20 12 0	5 3 0	—	—	18	1
592	24 4 0	6 1 0	—	—	3	3
656	20 16 0	5 4 0	—	—	13	1
800	28 4 0	7 1 0	—	—	13	2
848	28 8 0	7 2 0	—	—	15	1
976	20 24 0	5 6 0	—	—	6	3
	Superlattice reflections HHL					
72	2 2 8		21	1	—	—
86	5 5 6		—	—	80	1
96	4 4 8	1 1 2	17	1	—	—
102	7 7 2		—	—	15	1
102	1 1 10		—	—	107	1
144	8 8 4	2 2 1	10	1	11	1
272	8 8 12	2 2 3	5	2	9	1
288	4 4 16	1 1 4	23	1	—	—
352	12 12 8	3 3 2	10	1	—	—
528	8 8 20	2 2 5	—	—	20	1
528	16 16 4	4 4 1	—	—	36	1
544	12 12 16	3 3 4	—	—	21	1
608	4 4 24	1 1 6	—	—	17	1
864	12 12 24	3 3 6	—	—	15	2
864	20 20 8	5 5 2	—	—	8	3
912	8 8 28	2 2 7	—	—	8	3
912	16 16 20	4 4 5	—	—	18	1
	Superlattice reflections HKL					
50	5 3 4		0	1	—	—
66	1 7 4		0	1	—	—
98	1 9 4		0	1	—	—
122	5 9 4		—	—	0	1
146	7 9 4		0	1	—	—
162	5 11 4		0	1	—	—
210	5 13 4		—	—	0	2
306	13 11 4		0	1	—	—
450	9 15 12		0	1	—	—
224	12 8 4	3 2 1	13	1	—	—
336	16 8 4	4 2 1	11	1	—	—
416	16 12 4	4 3 1	18	1	23	1
464	16 12 8	4 3 2	12	1	—	—
480	20 8 4	5 2 1	12	1	—	—
608	20 12 8	5 3 2	—	—	11	1
656	24 8 4	6 2 1	—	—	17	1
672	20 16 4	5 4 1	—	—	22	1
720	20 16 8	5 4 2	—	—	10	1
736	24 12 4	6 3 1	—	—	18	1
784	24 12 8	6 3 2	—	—	11	2
800	20 16 12	5 4 3	—	—	19	1
848	24 16 4	6 4 1	—	—	21	1
864	28 8 4	7 2 1	—	—	0	2
976	24 16 12	6 4 3	—	—	22	1
992	24 20 4	6 5 1	—	—	19	1
992	28 12 8	7 3 2	—	—	11	1
86	7 1 6		—	—	21	1
250	15 3 4		9	1	—	—

that all of the superlattice reflections we measured obey the special position extinction rules for the 12a or 12b sites in the $I\bar{4}3d$ space group.

Only 60 extra oxygen atoms (instead of 64 in U_4O_9) may be located in 12 U_6O_{37} clusters. This deficit of four oxygen atoms inside the large cell is compatible with our measured sample composition. We have set the atoms at the positions related Table III given in (*14*), with four, α, β, γ, δ, variable positional parameters. The 256 uranium atoms and the 572 oxygen atoms are respectively located in 7 and 14 special positions of the $I\bar{4}3d$ space group with one uranium atom placed at the origin. Only 168/256 U atoms and 384/572 O atoms are allowed to move along the $[100]_j$, $[110]_j$, and $[111]_j$ rows, with two parameters attributed to the U atoms and two others to the O atoms. The positions determined by Bevan *et al.* were used at the first step of the least-squares process using the XFLSN program; the R factor defined as above is $R = 0.091$ for 137 data including fundamental and superlattice reflections with $F_{obs} \geq 2$ sig(F_{obs}). The final displacement values are summarized as follow: $\alpha = 0.0013 \pm 0.0043$ for 24 U atoms along $[100]_j$, $\beta = -0.0039 \pm 0.0003$ for 48 U atoms along $[100]_j$, and for 96 U atoms along $[111]_j$, $\gamma = 0.0318 \pm 0.0007$ for 144 O atoms along $[110]_j$, and $\delta = 0.0058 \pm 0.0005$ for 240 O atoms along $[100]_j$.

The results, except for the δ parameter, are in good qualitative agreement with those obtained by Bevan *et al.* (*14*), namely $\alpha = 0.003$, $\beta = -0.004$, $\gamma = 0.032$, and $\delta = 0.01$. We obtained a better R factor from our neutron collection; however, it seems to us that further statistical analysis is necessary.

Statistical Models

As reported by Willis (*4*), a superstructure can be analyzed on the basis of an average cell. In the case of U_4O_9, the content of the 64 subcells, contained in the $4a \times 4a \times 4a$ cell, is superimposed. So, an averaged description of the actual structure is obtained, where occupation number of atomic sites and displacements along some directions are the refined parameters. Willis (*4*) showed that the average structure belongs to the space group $P\bar{4}3m$.

In a first step, we tested the Willis model above the transition temperature. That lead us to retain only the fundamental reflections and to take the space group $F\bar{4}3m$ for the reduced cell, following the process proposed by Willis for his neutron data collected at room temperature (*4*). In a second

TABLE III

LEAST-SQUARES REFINEMENT

Type of atom	Atomic coordinates in composite cell $F\bar{4}3m$			Site occupation number p	Average number of atoms in the reduced cell
U (4d)	$\frac{3}{4}$	$\frac{3}{4}$	$\frac{3}{4}$	1	4
Oa (4e)	0	0	0	0.64 ± 0.02	2.55 ± 0.08
Ob (4b)	$\frac{1}{2}$	$\frac{1}{2}$	$\frac{1}{2}$	0.95 ± 0.02	3.80 ± 0.08
O′ (48h)	$\frac{1}{4} + \varepsilon'$	$\frac{1}{4} + \varepsilon'$	$\frac{1}{4}$	0.054 ± 0.002	2.57 ± 0.01
O″ (16e)	$\frac{1}{4} + \varepsilon''$	$\frac{1}{4} + \varepsilon''$	$\frac{1}{4} + \varepsilon''$	$0.02_2 \pm 0.01$	0.36 ± 0.04
$\varepsilon' = 0.123 \pm 0.002$				$\varepsilon'' = 0.06_2 \pm 0.02$	
$B_U = 0.84 \pm 0.02$ Å^2				$B_O = 1.78 \pm 0.03$ Å^2	

Note. Reduced cell $F\bar{4}3m$. $R = 0.036$.

step, we introduced fundamental reflections and superlattice reflections, whose indices are multiples of four, to describe the reduced cell with its true $P\bar{4}3m$ space group obtained in reducing the supercell $4a$ of space group $I\bar{4}3d$ (*4*). In both cases, the indices H, K, L (corresponding to the supercell) in multiples of four are only retained (Table II) and replaced by $h = H/4$, $k = K/4$, $l = L/4$ later on.

$F\bar{4}3m$ average cell. This model requires placing normal oxygen and uranium atoms at Wyckoff sites 4a, 4b, and 4c of $F\bar{4}3m$ space group, respectively, corresponding to the positions they occupy in the fluorite-type cell as reported in Table III. Two other new positions (O′) and (O″) are available for oxygen atoms in 48 h (x,x,z) and 16e (x,x,x), respectively; these positional parameters allow displacements along [110] and [111] from the center of normal oxygen atom cubes set at 4c $(\frac{1}{4}, \frac{1}{4}, \frac{1}{4})$.

Nine parameters, including the overall scale factor were incorporated in the XFLSN refinement program, namely the four occupation numbers of the 4a, 4b, 48h, and 16e sites by oxygen atoms, two position parameters ε' and ε'', one isotropic temperature factor for uranium atoms, and one other constrained to be the same for all oxygen atoms. The R factor defined as above is $R = 0.036$ for 45 fundamental reflections (Orphée data collection). Table III shows the results of the calculation: the displacements of oxygen atoms from site 4c are equal to (0.95 ± 0.02) Å along [110] that is 12% of the (110) translation and to (0.6 ± 0.2) Å along [111] that is 6% of the [111] body diagonal. The reduced cell contains on average:

$$U_4O_{6.35\pm0.11}O'_{2.57\pm0.01}O''_{0.36\pm0.04}.$$

In this formula, O is the number of normal oxygen atoms. Note that the oxygen atom composition is not constrained to be equal to 9 in order to check the validity of this calculation.

$P\bar{4}3m$ average cell. Now we deal with an analysis of the fundamental and superlattice reflections whose indices are multiples of four. This treatment involves an adjustment of the atomic distribution of the $P\bar{4}3m$ Wyckoff sites, which is detailed in Table IV.

In contrast to the Willis analysis, the uranium atoms are placed at sites allowing relaxation along [111] directions. As previously explained, oxygen atoms placed at sites 12i (x,x,z), 24j (x,y,z), 4e (x,x,x) have the possibility of relaxing along [110] and [111] directions from the center of oxygen atom cubes. The isotropic temperature factors are kept to the previous values. At last, 22 adjustable parameters are incorporated in the XFLSN refinement program including uranium displacements, position parameters of 3(O′) and 2(O″) sites, and their occupation numbers. The results of this calculation are shown in Table IV; the R factor converged to 0.049 for 120 data, obtained by merging the fundamental reflections and the superlattice reflections of indices in multiples of four belonging to both data sets. As previously explained, the composition of oxygen atoms is not constrained in the refinement. The result,

$$U_4O_{6.42\pm0.29}O'_{2.71\pm0.20}O''_{0.22\pm0.17},$$

is in agreement with the previous one within one standard deviation. It is noticeable that the uranium displacements from the positions they occupy in the UO_2 cell are not significant. Comparing Tables III and IV we see similar displacements along [110], but an appreciably increasing estimated standard deviation for displacements and composition of the (O″) oxygen atoms.

Discussion

The experimental results do not favor the interstitial model. Willis (*4*) came to the same conclusion, but on the basis of main

TABLE IV

LEAST-SQUARES REFINEMENT

Type of atom	Atomic coordinates in composite cell $P\bar{4}3m$	Displacement (Å)	Site occupation number	Average number of atoms in the reduced cell
U (4e)	(0.7500 + 0.0008) ± 0.0006 (0.7500 + 0.0008) ± 0.0006 (0.7500 + 0.0008) ± 0.0006			4
Oa(1) (4e)	0.000 0.000 0.000		0.038 ± 0.002	0.91 ± 0.04
Oa(2) (24j)	0.500 0.500 0.000		0.065 ± 0.008	1.56 ± 0.20
Ob(1) (4e)	0.500 0.500 0.500		0.041 ± 0.003	0.98 ± 0.07
Ob(2) (24j)	0.500 0.000 0.000		0.124 ± 0.008	2.97 ± 0.19
O′(1) (12i)	(0.250 + 0.121) ± 0.004 (0.250 + 0.121) ± 0.004 (0.250 + 0.001) ± 0.009	0.93 ± 0.01	0.041 ± 0.005	0.98 ± 0.12
O′(2) (12i)	(0.750 + 0.129) ± 0.008 (0.750 + 0.129) ± 0.008 (0.250 + 0.005) ± 0.011	0.99 ± 0.02	0.017 ± 0.003	0.41 ± 0.07
O′(3) (24j)	(0.250 + 0.124) ± 0.007 (0.750 + 0.117) ± 0.006 (0.750 + 0.017) ± 0.011	0.97 ± 0.02	0.055 ± 0.006	1.32 ± 0.14
O″(1) (4e)	(0.250 + 0.127) ± 0.027 (0.250 + 0.127) ± 0.027 (0.250 + 0.127) ± 0.027	1.20 ± 0.08	0.0041 ± 0.0043	0.10 ± 0.10
O″(2) (12i)	(0.750 + 0.045) ± 0.098 (0.750 + 0.045) ± 0.098 (0.250 + 0.084) ± 0.166	0.57 ± 0.41	0.0052 ± 0.0062	0.12 ± 0.15

Note. Reduced cell $P\bar{4}3m$. $R = 0.049$.

reflection intensities measured at room temperature. Nevertheless, the failure of interstitial structure models could be due to the constrained positions, so it would be necessary to refine again all the positional parameters taken as free, before the final conclusion.

The change in intensities of fundamental reflections at the transition determined by an R_2 factor, $R_2 = \Sigma|k|F_{wj}| - |F_{bj}||/|\Sigma F_{bj}|$ reaches 11% where $|F_{wj}|$ are the structure factors measured by Willis (*4*) at room temperature and $|F_{bj}|$ are those we obtained at 120°C; k is the scale factor between both sets of data. Despite the relatively small magnitude of this change, the effect on the

occupation number of sites and the displacements along [111] is important.

Using neutron data collected at room temperature Willis (*4*) found displacements of oxygen of 0.86 and 1.05 Å along [110] and [111], and an averaged composition equal to:

$$U_4O_{7.08\pm0.08}O'_{1.16\pm0.16}O''_{0.76\pm0.12}.$$

The comparison between these averaged compositions suggests a wide rearrangement of oxygen atoms at the transition summarized as follows:

—The number of vacancies at sites occupied by normal oxygen atoms increased from 1.0 to 1.6 on an average per cell.

—The number of (O′) oxygen atoms is doubled and the magnitude of their displacement is slightly increased.

—The number of (O″) oxygen atoms is divided by two to three and does not represent more than 10–15% of the (O′) number.

Nearly 18% of the normal oxygen atoms are ejected from the positions they occupy in the U_4O_8 fluorite structure above the transition temperature. Roughly, with respect to the average composition U_4O_8 + O, there are two fluorite-type oxygen vacancies and three oxygen atoms distributed in two new sites (O′) and (O″), in 90% proportion for (O′) and 10% for (O″).

A good qualitative agreement is obtained between the model of discrete U_6O_{37} groups and the $P\bar{4}3m$ averaged unit cell, as regards

—the proportion of oxygen vacancies: 8 per each group, that is, 17% in the large cell and 18% in the averaged cell; and

—the proportion of the (O′) oxygen atoms displaced in planes perpendicular to the $\bar{4}$ axis ([110] rows): 12 per each group, that is, 25% in the large cell, to compare with the (30 ± 2)% determined in the averaged cell; these displacements are equal to 1 Å within the limits of the errors.

On the other hand, the comparison of the displacements and the composition of the (O″) oxygen atoms is rather difficult due to the lack of precision. The displacements obtained on the average along [111] from the δ value are of an order of 0.2 Å and have an effect on 10% oxygen atoms. Roughly, the (O″) oxygen atoms can be neglected, taking into account the small value of their displacements. In addition, the uranium atoms do not actually move.

In hyperstoichiometric UO_{2+x}, U^{4+} is oxidized to U^{5+} and U^{6+} with a charge balance maintained by formation of a complex containing (O′) and (O″) interstitial oxygen atoms and vacancies in the normal oxygen sites. This appreciably reduced number of (O″) oxygen atoms makes unlikely the 2 : 2 : 2 defect cluster, which contains two (O′), two vacancies in the oxygen sublattice, and two (O″), as Willis (*21*) proposed for $UO_{2.12}$ on the basis of neutron diffraction results. Apparently, our experimental results fit better any defect complex where the number of vacancies is much greater than the number of (O″) oxygen atoms.

Recently, Allen and Tempest (*22*) Proposed mixtures of 4 : 3 : 2 clusters (4 O′ oxygen interstitials, along [110]; 3 oxygen vacancies; 2 O″ oxygen interstitials along [111]) and 2 : 2 : 2 clusters in highly oxidized uranium crystals. With regard to U_4O_9, they believe the distribution of oxygen interstitials can be pictured as linear ordered chains of 2 : 2 : 2 and 4 : 3 : 2 clusters.

In the fluorite-type structure, the introduction of extra anions involves only small displacements of the cations, according to Aleonard *et al.* (*12*). This is in agreement with the small uranium displacements which are obtained from the analysis based on $P\bar{4}3m$ average cell, and also on the cluster model. Nevertheless, the intensity increase of superlattice reflections as the Bragg angles on an X-ray Debye–Sherrer photograph suggests an ordered displacement of uranium atoms.

Concluding Remarks

Although X-ray Debye–Sherrer photographs show an obvious relationship between UO_2 and U_4O_9, it seems that U_4O_9 phase cannot be interpreted as a simple ordering of oxygen atoms in the vacant sites of the UO_2 fluorite structure.

The most uniform distribution of the extra oxygen atom in the UO_2 cell (exactly one per cell at the same site, space group $Pm3m$) is not observed. Consequently, some parts of the superlattice cell have an oxygen packing very dense, so that oxygen atom clusters probably exist, but the published models are moderately successful in describing the cluster structure.

The uranium displacements are found to be very small with respect to the oxygen displacements. Apparently this result is not in agreement with the fact that the intensity of superlattice reflections increases with the Bragg angles, as shown on an X-ray Debye–Scherrer photograph. As a matter of fact, this observation suggests an ordered displacement of uranium atoms. An anomalous X-ray diffraction experiment would improve the determination of the uranium atom contribution to the superlattice reflections.

Appendix

A heating system by blowing a stream of hot gas on the crystal has been constructed. This setup is designed for measurements over long periods on a single 4-circle diffractometer, between room temperature and 300°C. The system consists of double gas streams flowing coaxially; the central stream goes from a 6-mm-diameter nozzle, and the outer "cold" stream shields the inner warm stream against any turbulence in the laboratory. The gas flow and the temperature just after heating resistances are both regulated. With regard to a 10 liters/min air flow and in a range 10 to 20 mm from the nozzle, the temperature homogeneity is within 1°C in the air stream. Calibration of the air stream temperature as a function of the regulator temperature has been performed using a 10 liter/min air flow 15 mm away from the nozzle. The observed long-term stability is within ±1°C. It is believed that the sample, placed in the same manner as the microcalibrating platinium thermometer in the air stream, reaches an equilibrium temperature equal to the stream temperature after 10 min. A simple air pump with an additional buffer wessel or the compressed air supply with filters serves as the source of gas. Water cooling is not necessary. So, this heating system, mounted on a foot with adequate adjustment movements, provides easy and rapid setup. In conclusion, this equipment, which can be installed far enough from the neutron incident beam, does not introduce any parasitic diffusion. This feature favors the search of very weak reflections from the background.

Acknowledgments

The authors thank Professor P. Perio and B. Belbeoch for their valuable discussions and their helpful comments on the manuscript. Thanks are due to A. Vasset for the DSC measurements and to P. Schweiss for his kind assistance with neutron diffraction in L.L.B..

References

1. Technical Report IAEA, Vienne (1965).
2. B. Belbeoch, "Nouveau Traité de Chimie Minérale," Tome 15, 4ème fascicule, 626 (1967).
3. B. Belbeoch, C. Piekarski, and P. Perio, *Acta Crystallogr.* **14,** 837–843 (1961).
4. B. T. M. Willis, *J. Phys. Radium* **25,** 431–439 (1964).
5. H. Blank and C. Ronchi, *Acta Crystallogr. Sect. A* **24,** 657–666 (1968).
6. B. Belbeoch, J. C. Boivineau, and P. Perio, *J. Phys. Chem. Solids* **28,** 1267–1275 (1967).
7. K. Naito, T. Ishii, Y. Hamaguchi, and K. Oshima, *Solid State Commun.* **5,** 349–352 (1967).

8. K. GOTOO AND K. NAITO, *J. Phys. Chem. Solids* **26,** 1673–1677 (1965).
9. C. MAZIERES, private communication (1968).
10. N. MASAKI AND K. DOI, *Acta Crystallogr. Sect. B* **28,** 785–791 (1972).
11. N. MASAKI, *J. Appl. Crystallogr.* **7,** 247–250 (1974).
12. S. ALEONARD, Y. LE FUR, L. PONTONNIER, M. F. GORIUS, AND M. T. ROUX, *Ann. Chim.* **3,** 417–427 (1978).
13. D. J. M. BEVAN, O. GREIS, AND J. STRAHLE, *Acta Crystallogr. Sect. A* **36,** 889–890 (1980).
14. D. J. M. BEVAN, I. E. GREY AND B. T. M. WILLIS, *J. Solid State Chem.* **61,** 1–7 (1986).
15. A. VASSET, private communication (1985).
16. N. MASAKI AND K. DOI, *Acta Crystallogr. Sect. B* **24,** 1393–1394 (1968).
17. P. J. BROWN AND J. C. MATTHEWMAN, The Cambridge Crystallography Subroutine Library, RL-81-063 (1981).
18. K. D. ROUSE, B. T. M. WILLIS, AND A. W. PRYOR, *Acta Crystallogr. Sect. B* **24,** 117–122 (1968).
19. P. PERIO, private communication (1985).
20. W. R. BUSING, K. O. MARTIN, AND H. A. LEVY, ORXFLS 3, Report ORNL, 59-4-39 Oak Ridge National Laboratory, Oak Ridge, TN (1971).
21. B. T. M. WILLIS, *Acta Crystallogr. Sect. A* **34,** 88–90 (1978).
22. G. C. ALLEN AND P. A. TEMPEST, *J. Chem. Soc. Dalton Trans.*, 2673–2677 (1983).